5. Supplementary Appendix

Positivity and boundedness of the solution for the Model (2.2)

This subsection is provided to prove the positivity and boundedness of solutions of the system (2.2) with initial conditions $(S(0), L(0), E(0), A(0), I(0), C(0), R(0))^T \in \mathbb{R}^7_{+0}$. We first state the following lemma.

Lemma 5.1. *Suppose* $\Omega \subset \mathbb{R}\times\mathbb{C}^n$ *is open,* $f_i \in C(\Omega, \mathbb{R}), i = 1, 2, 3, ..., n$. *If* $f_i|_{x_i(t)=0, X_t\in\mathbb{C}^n_{+0}} \geq 0$, $X_t = (x_{1t}, x_{2t}, ..., x_{1n})^T, i = 1, 2, 3, ..., n$, *then* $\mathbb{C}^n_{+0}\{\phi = (\phi_1, ..., \phi_n) : \phi \in \mathbb{C}([-\tau, 0], \mathbb{R}^n_{+0})\}$ *is the invariant domain of the following equations*

$$\frac{dx_i(t)}{dt} = f_i(t, X_t), t \geq \sigma, i = 1, 2, 3, ..., n.$$

where $\mathbb{R}^n_{+0} = \{(x_1, ...x_n) : x_i \geq 0, i = 1, ..., n\}$ *[39].*

Proposition 5.1. *The system* (2.2) *is invariant in* $\mathbb{R}^7_{+0}$.

Proof. By re-writing the system (2.2) we have:

$$\frac{dX}{dt} = B(X(t)), X(0) = X_0 \geq 0 \qquad \text{(S-1)}$$

$B(X(t)) = (B_1(X), B_1(X), ..., B_7(X))^T$

We note that

$$\frac{dS}{dt}|_{S=0} = \Pi_H + \omega L > 0, \frac{dL}{dt}|_{L=0} = lS \geq 0, \frac{dE}{dt}|_{E=0} = \frac{\beta_1 S(I + \rho A)}{N - C} \geq 0,$$
$$\frac{dA}{dt}|_{A=0} = (1 - \kappa)\sigma E \geq 0, \frac{dI}{dt}|_{I=0} = \kappa\sigma E \geq 0, \frac{dC}{dt}|_{C=0} = \tau I \geq 0,$$
$$\frac{dR}{dt}|_{R=0} = \gamma_1 A + \gamma_2 I + \gamma_3 C \geq 0.$$

Then it follows from the Lemma 5.1 that $\mathbb{R}^7_{+0}$ is an invariant set for the COVID-19 system (2.2) with lockdown. □

Corollary 5.1. *The system* (2.1) *is invariant in* $\mathbb{R}^6_{+0}$.

Proof. Proceeding as proposition 5.1, we can easily show that $\mathbb{R}^6_{+0}$ is an invariant set for the COVID-19 system (2.1) without lockdown. □

Lemma 5.2. *The system* (2.2) *is bounded in the region* $\Omega = \{(S, L, E, A, I, C, R) \in \mathbb{R}^7_{+0}|S + L + E + A + I + C + R \leq \frac{\Pi_H}{\mu}\}$

Proof. We have from the system (2.2):

$$\frac{dN}{dt} = \Pi_H - \mu N - \delta C \leq \Pi_H - \mu N$$
$$\implies \lim_{t\to\infty} sup N(t) \leq \frac{\Pi_H}{\mu}$$

Hence the system (2.2) is bounded. □

Corollary 5.2. *The system* (2.1) *is bounded in the region* $\Omega^* = \{(S, E, A, I, C, R) \in \mathbb{R}^6_{+0} | S + E + A + I + C + R \leq \frac{\Pi_H}{\mu}\}$

Proof. proceeding same as lemma 5.2, we can easily show that the system (2.1) is bounded in Ω^*. □

Local stability of disease-free equilibrium (DFE)

The DFE of the model (2.2) is provided as follows:

$$\begin{aligned}\varepsilon_0 &= (S^0, L^0, E^0, A^0, I^0, C^0, R^0)\\ &= \Big(\frac{\Pi_H(\mu+\omega)}{\mu\,(\mu+\omega+l)}, \frac{\Pi_H l}{\mu\,(\mu+\omega+l)}, 0, 0, 0, 0, 0\Big)\end{aligned}$$

The local stability of ε_0 can be established for the COVID-19 system (2.2) by using the next generation operator method. Using the notation in [32], the matrices F for the new infection and V for the transition terms are given, respectively, by

$$F = \begin{pmatrix} 0 & \rho\beta_1 & \beta_1 & 0 \\ 0 & 0 & 0 & 0 \\ 0 & 0 & 0 & 0 \\ 0 & 0 & 0 & 0 \end{pmatrix},$$

$$V = \begin{pmatrix} \mu+\sigma & 0 & 0 & 0 \\ -(1-\kappa)\sigma & \gamma_1+\mu & 0 & 0 \\ -\kappa\sigma & 0 & \gamma_2+\tau+\mu & 0 \\ 0 & 0 & -\tau & \delta+\gamma_3+\mu \end{pmatrix}.$$

It follows that the basic reproduction number [40], denoted by $R_0 = \Phi(FV^{-1})$, where Φ is the spectral radius, is given by

$$R_0 = \frac{\beta_1\kappa\sigma}{(\mu+\sigma)(\gamma_2+\tau+\mu)} + \frac{\rho\beta_1(1-\kappa)\sigma}{(\mu+\sigma)(\gamma_1+\mu)}$$

Using Theorem 2 in [32], the following result is established.

Lemma 5.3. *The DFE,* ε_0*, of the model* (2.2) *is locally-asymptotically stable (LAS) if* $R_0 < 1$*, and unstable if* $R_0 > 1$.

The threshold quantity, R_0 is the basic reproduction number of the disease [40; 41; 42]. This represent the average number of secondary cases generated by a infected person in a fully susceptible population. The epidemiological significance of 5.3 is that when R_0 is less than unity, a low influx of infected individuals into the population will not cause major outbreaks, and the disease would die out in time.

Global stability of DFE

Theorem 5.1. *The DFE of the model* (2.2) *is globally asymptotically stable in* Ω *whenever* $R_0 \leq 1$.

Proof. Consider the following Lyapunov function

$$\mathcal{L} = \Big(\frac{\sigma(\kappa k_2 + \rho(1-\kappa)k_3)}{k_1 k_2}\Big)E + \Big(\frac{\rho k_3}{k_2}\Big)A + I$$

where $k_1 = \mu + \sigma$, $k_2 = \gamma_1 + \mu$ and $k_3 = \gamma_2 + \tau + \mu$.
We take the Lyapunov derivative with respect to t,

$$\begin{aligned}
\dot{\mathcal{L}} &= \Big(\frac{\sigma(\kappa k_2 + \rho(1-\kappa)k_3)}{k_1 k_2}\Big)\dot{E} + \Big(\frac{\rho k_3}{k_2}\Big)\dot{A} + \dot{I} \\
&= \frac{\sigma(\kappa k_2 + \rho(1-\kappa)k_3)}{k_1 k_2}\Big[\frac{\beta_1 S(I+\rho A)}{N-L-C} - k_1 E\Big] + \frac{\rho k_3}{k_2}[(1-\kappa)\sigma E - k_2 A] + (\kappa\sigma E - k_3 I) \\
&\leq \frac{\beta_1\sigma(\kappa k_2 + \rho(1-\kappa)k_3)}{k_1 k_2}(I+\rho A) - \frac{\sigma(\kappa k_2 + \rho(1-\kappa)k_3)}{k_2}E + \frac{\rho(1-\kappa)k_3\sigma}{k_2}E \\
&\quad - \rho k_3 A + \kappa\sigma E - k_3 I \text{ (Since } S \leq N-L-C \text{ in } \Omega) \\
&= \frac{\beta_1\sigma(\kappa k_2 + \rho(1-\kappa)k_3)}{k_1 k_2}(I+\rho A) - \rho k_3 A - k_3 I \\
&= \frac{\beta_1\sigma(\kappa k_2 + \rho(1-\kappa)k_3)}{k_1 k_2 k_3}k_3(I+\rho A) - \rho k_3 A - k_3 I \\
&\leq k_3(R_0 - 1)(I+\rho A) \leq 0, \text{ whenever } R_0 \leq 1.
\end{aligned}$$

Since all the variables and parameters of the model (2.2) are non-negative, it follows that $\dot{\mathcal{L}} \leq 0$ for $R_0 \leq 1$ with $\dot{\mathcal{L}} = 0$ at diseases free equilibrium. Hence, $\mathcal{L}$ is a Lyapunov function on Ω. Therefore, followed by LaSalles Invariance Principle [43], that

$$(E(t), A(t), I(t)) \to (0,0,0) \text{ as } t \to \infty \tag{S-2}$$

Since $\lim\limits_{t\to\infty} supI(t) = 0$ (from S-2), it follows that, for sufficiently small $\epsilon > 0$, there exist constants $B_1 > 0$ such that $\lim\limits_{t\to\infty} supI(t) \leq \epsilon$ for all $t > B_1$.
Hence, it follows from the sixth equation of the model (2.2) that, for $t > B_1$,

$$\frac{dC}{dt} \leq \tau\epsilon - k_4 C$$

Therefore using comparison theorem [44]

$$C^\infty = \lim_{t\to\infty} supC(t) \leq \frac{\tau\epsilon}{k_4}$$

So as $\epsilon \to 0$, $C^{\infty} = \lim_{t\to\infty} sup C(t) \leq 0$
Similarly by using $\lim_{t\to\infty} inf I(t) = 0$, it can be shown that

$$C_{\infty} = \lim_{t\to\infty} inf C(t) \geq 0$$

Thus, it follows from above two relations

$$C_{\infty} \geq 0 \geq C^{\infty}$$

Hence $\lim_{t\to\infty} C(t) = 0$
Similarly, it can be shown that

$$\lim_{t\to\infty} R(t) = 0, \lim_{t\to\infty} S(t) = \frac{\Pi_H (\mu + \omega)}{\mu (\mu + \omega + l)}, \text{and} \lim_{t\to\infty} L(t) = \frac{\Pi_H l}{\mu (\mu + \omega + l)}.$$

Therefore by combining all above equations, it follows that each solution of the model equations (2.2), with initial conditions $\in \Omega$, approaches ε_0 as $t \to \infty$ for $R_0 \leq 1$. □

Existence and stability of endemic equilibria

In this section, the existence of the endemic equilibrium of the model (2.2) is established. Let us denote

$$M_1 = \frac{\mu + \omega}{\mu + \sigma}, M_2 = \frac{(1-\kappa)\sigma(\mu + \omega)}{(\mu + \gamma_1)(\mu + \sigma)}, M_3 = \frac{\kappa\sigma(\mu + \omega)}{(\mu + \gamma_2 + \tau)(\mu + \sigma)},$$
$$M_4 = \frac{\kappa\tau\sigma(\mu + \omega)}{(\mu + \gamma_2 + \tau)(\mu + \gamma_3 + \delta)(\mu + \sigma)}.$$

Let $\varepsilon^* = (S^*, E^*, A^*, I^*, C^*, R^*)$ represents any arbitrary endemic equilibrium point (EEP) of the model (2.2). Further, define

$$\lambda^* = \frac{\beta_1(I^* + \rho A^*)}{N^* - L^* - C^*} \tag{S-3}$$

It follows, by solving the equations in (2.2) at steady-state, that

$$S^* = \frac{(\mu + \omega) L^*}{l}, L^* = \frac{\Pi_H l}{\lambda^* (\mu + \omega) + \mu (\mu + \omega + l)}, E^* = \frac{M_1 L^* \lambda^*}{l}, \tag{S-4}$$
$$A^* = \frac{M_2 L^* \lambda^*}{l}, I^* = \frac{M_3 L^* \lambda^*}{l}, C^* = \frac{M_4 L^* \lambda^*}{l}$$
$$R^* = \frac{(\gamma_1 M_2 + \gamma_2 M_3 + \gamma_3 M_4) L^* \lambda^*}{l\mu}$$

Substituting the expression in (S-4) into (S-3) shows that the non-zero equilibrium of the model (2.1) satisfy the following linear equation, in terms of λ^*:

$$A\lambda^* = B \tag{S-5}$$

where

$$\begin{aligned} A &= \mu M_1 + M_2(\mu + \gamma_1) + M_3(\mu + \gamma_2) + \gamma_3 M_4 \\ B &= \mu(\mu + \omega)(R_0 - 1) \end{aligned}$$

Since, $M_1 > 0$, $M_2 > 0$, $M_3 > 0$, and $M_4 > 0 \implies A > 0$, it is clear that the model (2.2) has an unique endemic equilibrium point (EEP) whenever $R_0 > 1$ and no positive endemic equilibrium point whenever $R_0 < 1$. This rules out the possibility of the existence of equilibrium other than DFE whenever $R_0 < 1$. Therefore, we have the following result:

Theorem 5.2. *The model* (2.2) *has a unique endemic (positive) equilibrium, given by* ε^**, whenever* $R_0 > 1$ *and has no endemic equilibrium for* $R_0 \leq 1$.

Now we will prove the local stability of endemic equilibrium.

Theorem 5.3. *The endemic equilibrium* ε^* *of the COVID-19 system* (2.2) *with lockdown is locally asymptotically stable if* $R_0 > 1$.

Proof. The Jacobian matrix of the system (2.2) J_{ε_0} at DFE is given by

$$J_{\varepsilon_0} = \begin{pmatrix} -(\mu + l) & \omega & 0 & -\rho\beta_1 & -\beta_1 & 0 & 0 \\ l & -(\mu + \omega) & 0 & 0 & 0 & 0 & 0 \\ 0 & 0 & -(\mu + \sigma) & \rho\beta_1 & \beta_1 & 0 & 0 \\ 0 & 0 & (1 - \kappa)\sigma & -(\mu + \gamma_1) & 0 & 0 & 0 \\ 0 & 0 & \kappa\sigma & 0 & -(\mu + \gamma_2 + \tau) & 0 & 0 \\ 0 & 0 & 0 & 0 & \tau & -(\mu + \gamma_3 + \delta) & 0 \\ 0 & 0 & 0 & \gamma_1 & \gamma_2 & \gamma_3 & -\mu \end{pmatrix},$$

Here, by taking β_1 as a bifurcation parameter, we use the central manifold theory method to determine the local stability of the endemic equilibrium [45]. Taking β_1 as the bifurcation parameter and gives critical value of β_1 at $R_0 = 1$ is given as

$$\beta_1^* = \frac{(\mu + \sigma)(\gamma_1 + \mu)(\gamma_2 + \tau + \mu)}{[\kappa\sigma(\gamma_1 + \mu) + (1 - \kappa)\rho\sigma(\gamma_2 + \tau + \mu)]}$$

The Jacobian of (2.2) at $\beta = \beta_1^*$, denoted by $J_{\varepsilon_0}|_{\beta=\beta_1^*}$ has a right eigenvector (corresponding to the zero eigenvalue) given by $w = (w_1, w_2, w_3, w_4, w_5, w_6, w_7)^T$, where

$$w_1 = -\frac{(\mu+\sigma)(\mu+\omega)}{\mu(\mu+\omega+l)}, w_2 = -\frac{(\mu+\sigma)\, l}{\mu(\mu+\omega+l)}, w_3 = 1, w_4 = \frac{(1-\kappa)\sigma}{\mu+\gamma_1},$$
$$w_5 = \frac{\kappa\sigma}{\mu+\gamma_2+\tau}, w_6 = \frac{\kappa\sigma\tau}{(\mu+\gamma_2+\tau)(\mu+\gamma_3+\delta)}$$
$$w_7 = \frac{\gamma_1(1-\kappa)\sigma}{\mu(\gamma_1+\mu)} + \frac{\gamma_2\kappa\sigma}{\mu(\gamma_2+\tau+\mu)} + \frac{\gamma_3\tau\kappa\sigma}{\mu(\gamma_2+\tau+\mu)(\delta+\gamma_3+\mu)}$$

Similarly, from $J_{\varepsilon_0}|_{\beta=\beta_1^*}$, we obtain a left eigenvector $v = (v_1, v_2, v_3, v_4, v_5, v_6, v_7)$ (corresponding to the zero eigenvalue), where

$$v_1 = 0, v_2 = 0, v_3 = 1, v_4 = \frac{\rho\beta_1^*}{\gamma_1+\mu}, v_5 = \frac{\beta_1^*}{\gamma_2+\tau+\mu}, v_6 = 0, v_7 = 0.$$

Selecting the notations $S = x_1$, $L = x_2$, $E = x_3$, $A = x_4$, $I = x_5$, $C = x_6$, $R = x_7$ and $\frac{dx_i}{dt} = f_i$. Now we calculate the following second-order partial derivatives of f_i at the disease-free equilibrium ε_0 and obtain

$$\frac{\partial^2 f_3}{\partial x_4 \partial x_3} = -\frac{\rho\beta_1^*\mu(\mu+\omega+l)}{\Pi_H(\mu+\omega)} = \frac{\partial^2 f_2}{\partial x_3 \partial x_4},$$
$$\frac{\partial^2 f_3}{\partial x_5 \partial x_3} = -\frac{\beta_1^*\mu(\mu+\omega+l)}{\Pi_H(\mu+\omega)} = \frac{\partial^2 f_3}{\partial x_3 \partial x_5},$$
$$\frac{\partial^2 f_3}{\partial x_4^2} = -\frac{2\rho\beta_1^*\mu(\mu+\omega+l)}{\Pi_H(\mu+\omega)},$$
$$\frac{\partial^2 f_3}{\partial x_5^2} = -\frac{2\beta_1^*\mu(\mu+\omega+l)}{\Pi_H(\mu+\omega)},$$
$$\frac{\partial^2 f_3}{\partial x_4 \partial x_5} = -\frac{(1+\rho)\beta_1^*\mu(\mu+\omega+l)}{\Pi_H(\mu+\omega)} = \frac{\partial^2 f_3}{\partial x_5 \partial x_4},$$
$$\frac{\partial^2 f_3}{\partial x_7 \partial x_4} = -\frac{\rho\beta_1^*\mu(\mu+\omega+l)}{\Pi_H(\mu+\omega)} = \frac{\partial^2 f_3}{\partial x_4 \partial x_7},$$
$$\frac{\partial^2 f_3}{\partial x_7 \partial x_5} = -\frac{\beta_1^*\mu(\mu+\omega+l)}{\Pi_H(\mu+\omega)} = \frac{\partial^2 f_3}{\partial x_5 \partial x_7}.$$

Now we calculate the coefficients a and b defined in Theorem 4.1 [45] of Castillo-Chavez and Song as follow

$$a = \sum_{k,i,j=1}^{6} v_k w_i w_j \frac{\partial^2 f_k(0,0)}{\partial x_i \partial x_j}$$

and

$$b = \sum_{k,i=1}^{6} v_k w_i \frac{\partial^2 f_k(0,0)}{\partial x_i \partial \beta}$$

Replacing the values of all the second-order derivatives measured at DFE and $\beta_1 = \beta_1^*$, we get

$$a = -2\left(w_3 + w_4 + w_5 + w_7\right)\left[\frac{\rho\beta_1^*\mu\left(\mu+\omega+l\right)}{\Pi_H\left(\mu+\omega\right)}w_4 + \frac{\beta_1^*\mu\left(\mu+\omega+l\right)}{\Pi_H\left(\mu+\omega\right)}w_5\right] < 0$$

and

$$\begin{aligned} b &= \rho w_4 + w_5 \\ &= \frac{\left(1-\kappa\right)\sigma\rho}{\left(\mu+\gamma_1\right)} + \frac{\kappa\sigma}{\left(\mu+\gamma_2+\tau\right)} > 0. \end{aligned}$$

Since $a < 0$ and $b > 0$ at $\beta = \beta_1^*$, therefore using the Remark 1 of the Theorem 4.1 stated in [45], a transcritical bifurcation occurs at $R_0 = 1$ and the unique endemic equilibrium of the COVID-19 system (2.2) with lockdown is locally asymptotically stable for $R_0 > 1$. $\square$

Figures

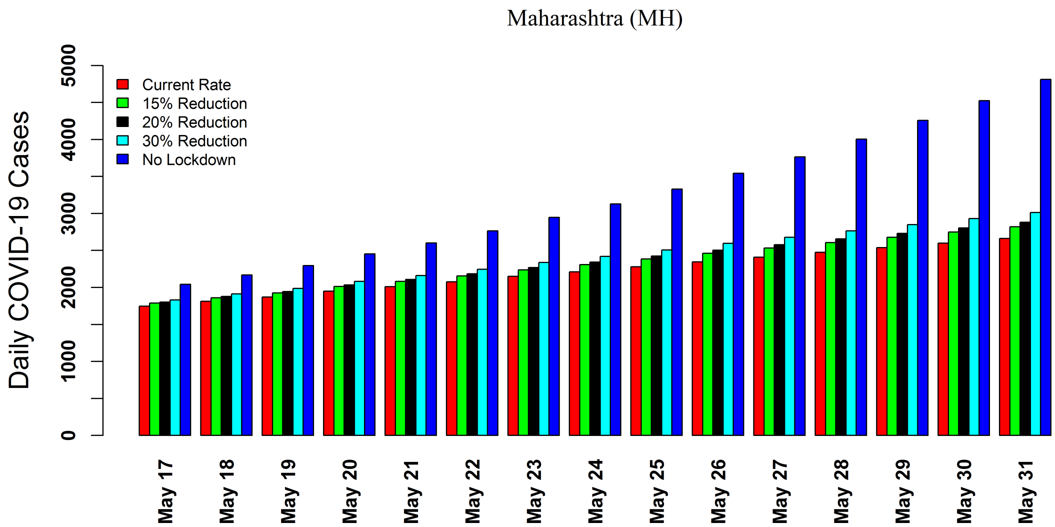

Figure S1: Ensemble model forecast for the daily notified COVID-19 cases in Maharashtra during May 17, 2020 till May 31, 2020, under five different social distancing measure. Various legends are **Current Rate**: daily notified case projection using the estimated value of the lockdown rate (see Table 4 main text), **15% Reduction**: daily notified case projection using 15% reduction in the estimated value of the lockdown rate (see Table 4 main text), **20% Reduction**: daily notified case projection using 20% reduction in the estimated value of the lockdown rate (see Table 4 main text), **30% Reduction**: daily notified case projection using 30% reduction in the estimated value of the lockdown rate (see Table 4 main text), and **No lockdown**: daily notified case projection based on no lockdown scenario, respectively.

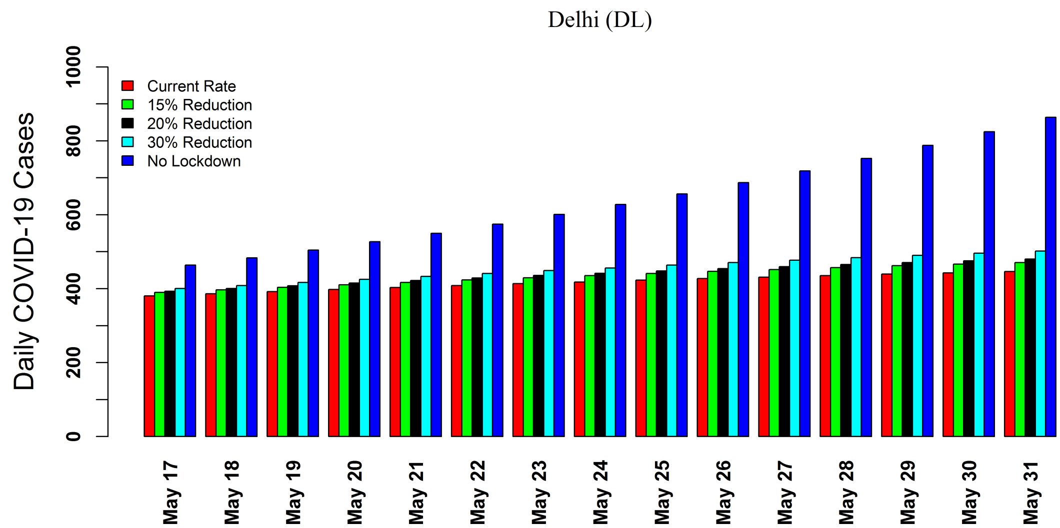

Figure S2: Ensemble model forecast for the daily notified COVID-19 cases in Delhi during May 17, 2020 till May 31, 2020, under five different social distancing measure. Various legends are same as Fig S1.

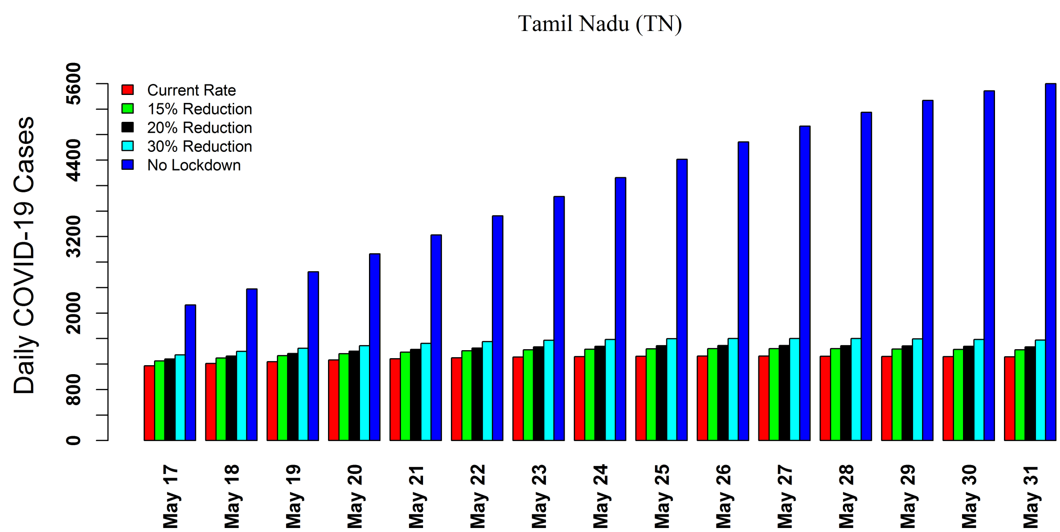

Figure S3: Ensemble model forecast for the daily notified COVID-19 cases in Tamil Nadu during May 17, 2020 till May 31, 2020, under five different social distancing measure. Various legends are same as Fig S1.

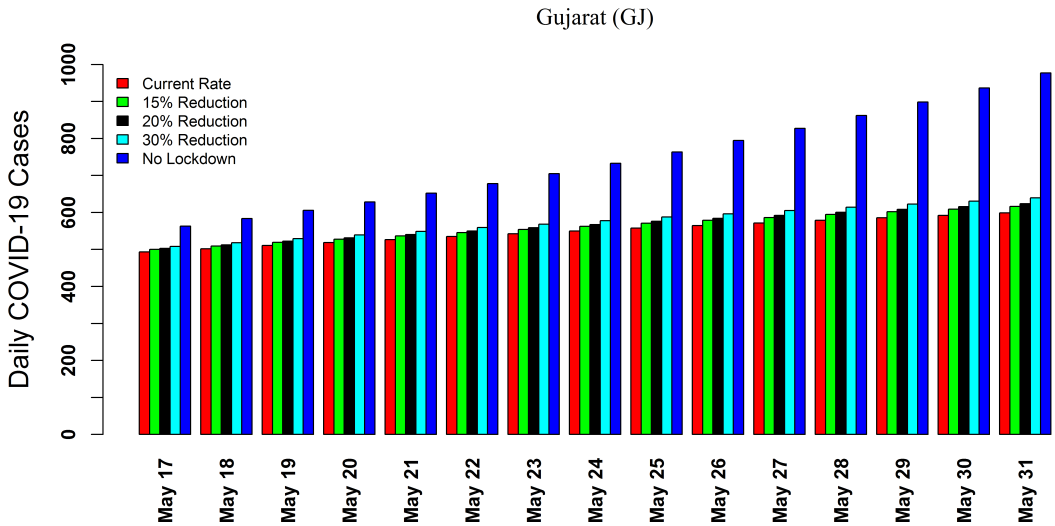

Figure S4: Ensemble model forecast for the daily notified COVID-19 cases in Gujarat during May 17, 2020 till May 31, 2020, under five different social distancing measure. Various legends are same as Fig S1.

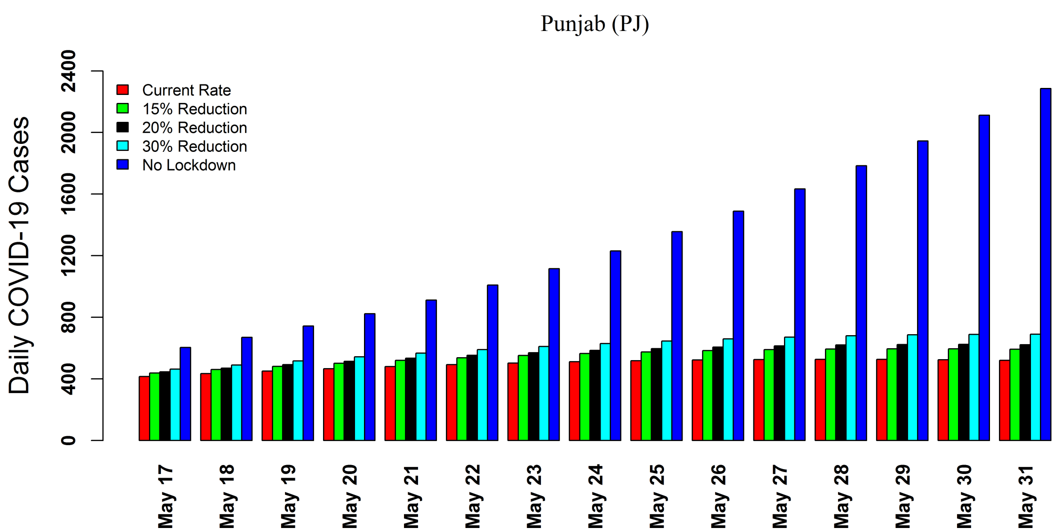

Figure S5: Ensemble model forecast for the daily notified COVID-19 cases in Punjab during May 17, 2020 till May 31, 2020, under five different social distancing measure. Various legends are same as Fig S1.

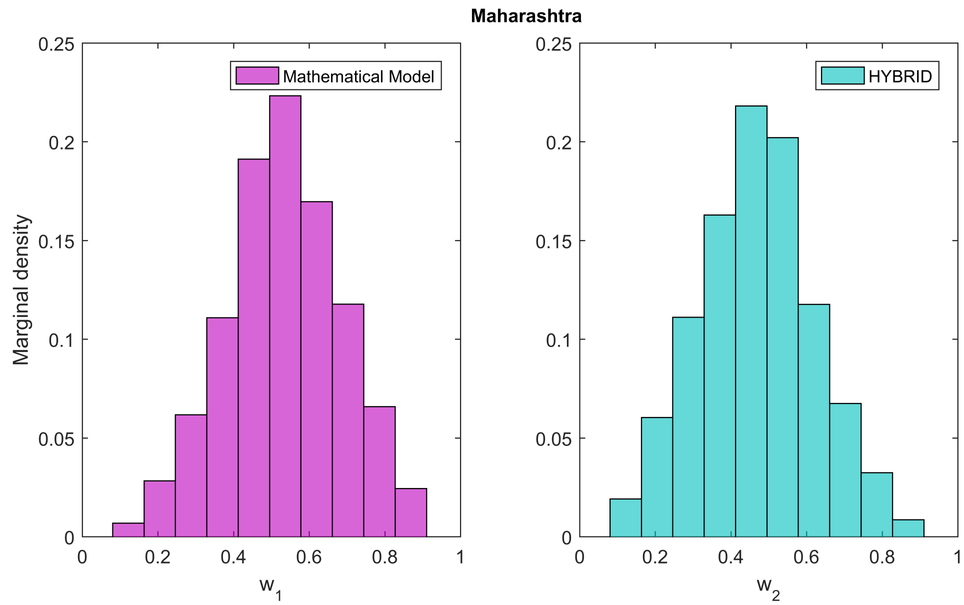

Figure S6: Posterior density of the weights for the mechanistic mathematical model (2.1 & 2.2) and the best statistical forecast model (HYBRID), respectively for Maharashtra.

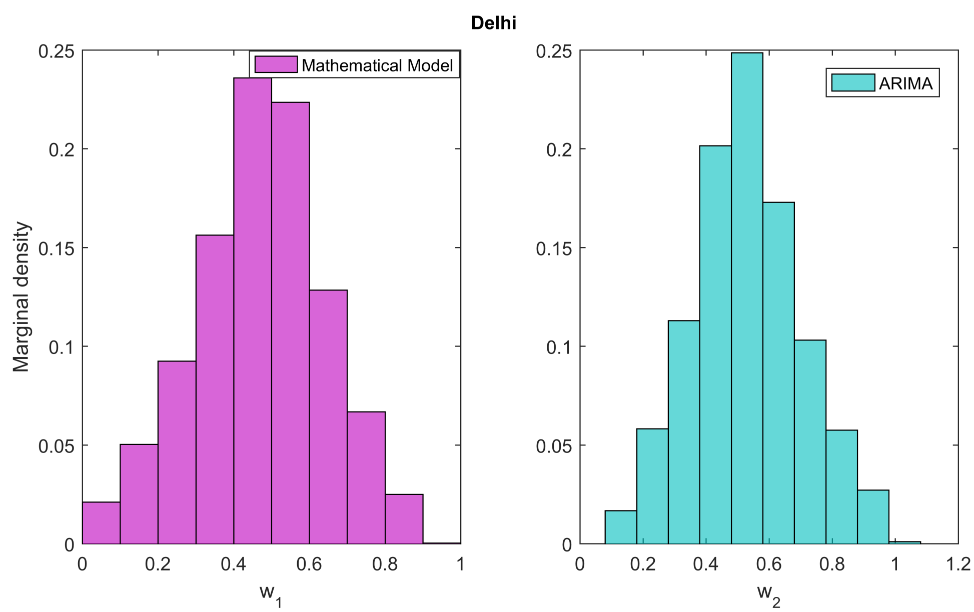

Figure S7: Posterior density of the weights for the mechanistic mathematical model (2.1 & 2.2) and the best statistical forecast model (ARIMA), respectively for Delhi

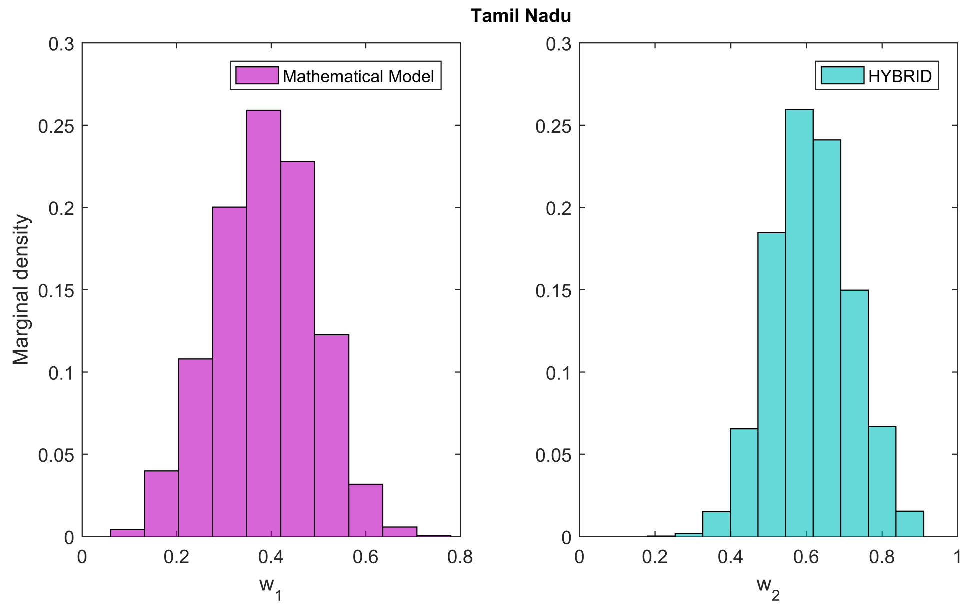

Figure S8: Posterior density of the weights for the mechanistic mathematical model (2.1 & 2.2) and the best statistical forecast model (HYBRID), respectively for Tamil Nadu.

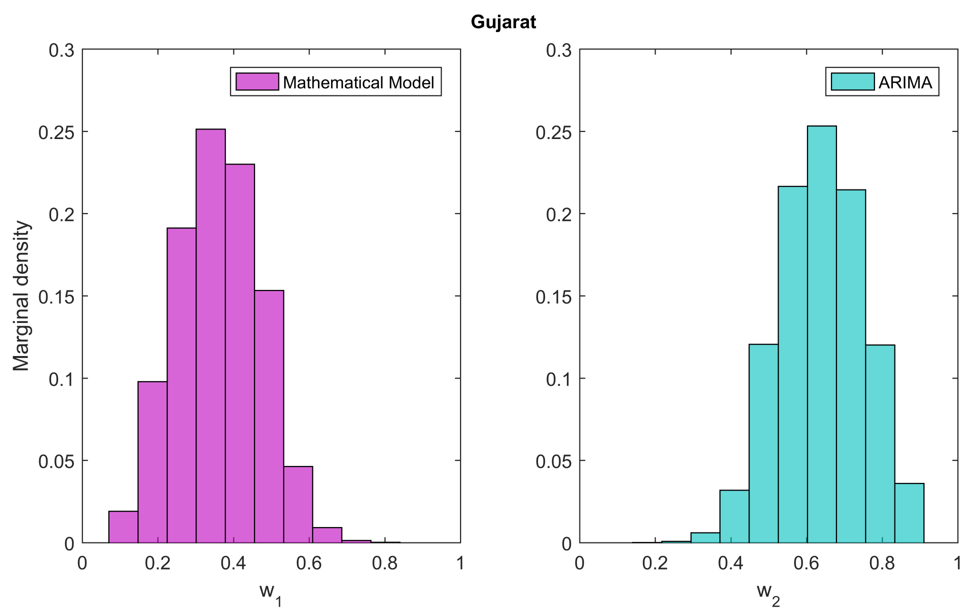

Figure S9: Posterior density of the weights for the mechanistic mathematical model (2.1 & 2.2) and the best statistical forecast model (ARIMA), respectively for Gujarat.

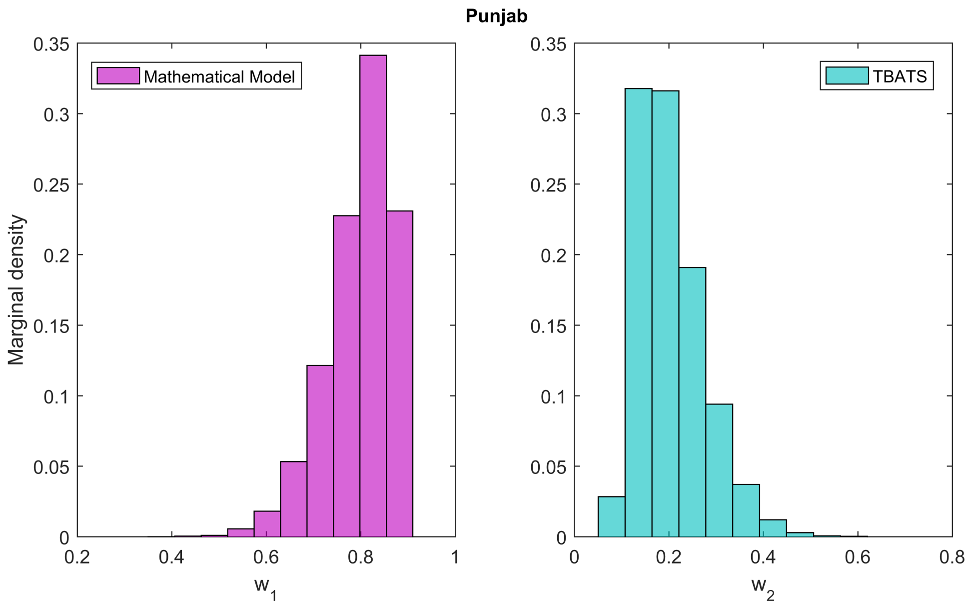

Figure S10: Posterior density of the weights for the mechanistic mathematical model (2.1 & 2.2) and the best statistical forecast model (TBATS), respectively for Punjab.

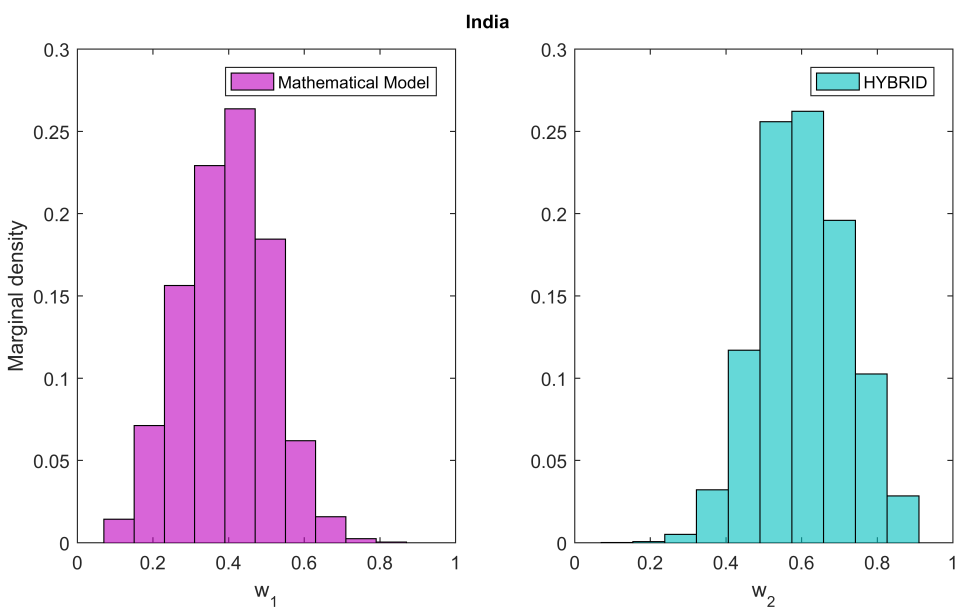

Figure S11: Posterior density of the weights for the mechanistic mathematical model (2.1 & 2.2) and the best statistical forecast model (HYBRID), respectively for India.

Tables

Table S1: Estimated initial state variables of the mathematical model (2.1). All data are given in the format **Estimate (95% CI)**.

Location	$S(0)$	$E(0)$	$A(0)$	$I(0)$
Maharashtra	123243118 (114977907−124511349)	27.27 (0.51−35.06)	9531 (9483−9989)	24.76 (14.17−30.26)
Delhi	16070717 (10346593−19737264)	14.74 (0.05−14.97)	437 (92.38−4017)	282 (7.82−325)
Tamil Nadu	75367306 (70335585−79738740)	4.80 (0.05−4.73)	0.40 (0.03−2.52)	7.61 (1.96−10.88)
Gujarat	66848292 (60218205−69744037)	7630 (2622−9775)	26.10 (1.26−28.70)	14.01 (0.02−20.54)
Punjab	26433551 (26433543−26433556)	7.83 (0.20−13.81)	19.26 (0.29−29.54)	8 (1.08−15.96)
India	1226841787 (1219848614−1297276832)	221104 (21136−279521)	462997 (27541−642484)	36043 (3601−84059)

Table S2: Goodness of fit (RMSE) for the three statistical forecast model (ARIMA, TBATS and HYBRID), respectively. RMSE for different locations are calculated only for the test period data (May 4, 2020 till May 8, 2020). RMSE values of the best performed statistical forecast model in different locations are shown in red.

Location	ARIMA	TBATS	HYBRID
Maharashtra	**179.84368**	**110.57237**	**90.04999**
Delhi	**92.17782**	**96.11452**	**94.14085**
Tamil Nadu	**182.5897**	**244.8254**	**119.9740**
Gujarat	**28.16381**	**37.36576**	**30.92572**
Punjab	**292.5078**	**188.9780**	**238.9491**
India	**457.7622**	**438.1160**	**368.0725**

Table S3: Weight estimates for the mechanistic mathematical model (2.1 & 2.2) and the best statistical forecast model, respectively. Respective subscript are MH: Maharashtra, DL: Delhi, TN: Tamil Nadu, GJ: Gujarat, PJ: Punjab, and IND: India. $\boldsymbol{w_1}$ and $\boldsymbol{w_2}$ denote the weights of the COVID-19 mathematical model (2.1 & 2.2) and the best statistical forecast model, respectively for a region. All data are provided in the format **Estimate (95% CI)**.

Weights	MH	DL	TN	GJ	PJ	IND
$\boldsymbol{w_1}$	0.48 (0.2243−0.8262)	0.5186 (0.1112−0.8004)	0.6158 (0.1801−0.5848)	0.2009 (0.1554−0.5737)	0.8331 (0.6291−0.8942)	0.3131 (0.1695−0.6149)
$\boldsymbol{w_2}$	0.52 (0.1738−0.7757)	0.4814 (0.1996−0.8888)	0.3842 (0.4152−0.8199)	0.7991 (0.4263−0.8446)	0.1669 (0.1058−0.3709)	0.6869 (0.3851−0.8305)

39. X Yang, L Chen, J Chen Permanence and positive periodic solution for the single-species nonautonomous delay diffusive models. Comput Math Appl 1996;32(4):109–116.

40. H W Hethcote The mathematics of infectious diseases. SIAM Rev 2000;42(4):599–653.

41. R M Anderson, R M May Population biology of infectious diseases: part i. Nature 1979;280(5721):361–367.

42. R M Anderson, B Anderson, R M May Infectious diseases of humans: dynamics and control. Oxford university press; 1992.

43. J.P. LaSalle The stability of dynamical systems 1976 Siam Vol. 25

44. H L Smith, P Waltman The theory of the chemostat: dynamics of microbial competition, vol. 13. Cambridge university press; 1995

45. C Castillo-Chavez, B Song Dynamical models of tuberculosis and their applications. Math Biosci Eng 2004;1(2):361.